IEEE Access
Multidisciplinary | Rapid Review | Open Access Journal

SPECIAL SECTION ON ADVANCES IN STATISTICAL CHANNEL MODELING FOR FUTURE WIRELESS COMMUNICATIONS NETWORKS

Received July 19, 2019, accepted August 5, 2019, date of publication August 12, 2019, date of current version August 22, 2019.

Digital Object Identifier 10.1109/ACCESS.2019.2934635

A Spatially Consistent MIMO Channel Model With Adjustable K Factor

STEFAN PRATSCHNER[1,2], (Student Member, IEEE), THOMAS BLAZEK[2], (Student Member, IEEE), ERICH ZÖCHMANN[1,2], (Member, IEEE), FJOLLA ADEMAJ[1,2], SEBASTIAN CABAN[2], STEFAN SCHWARZ[1,2], (Member, IEEE), AND MARKUS RUPP[2], (Fellow, IEEE)

[1]Christian Doppler Laboratory for Dependable Wireless Connectivity for the Society in Motion, TU Wien, Vienna 1040, Austria
[2]Institute of Telecommunications, TU Wien, Vienna, Austria

Corresponding author: Stefan Pratschner (stefan.pratschner@tuwien.ac.at)

This work was supported in part by the Christian Doppler Laboratory for Dependable Wireless Connectivity for the Society in Motion, in part by the Austrian Federal Ministry for Digital and Economic Affairs, in part by the National Foundation for Research, Technology, and Development, and in part by the TU Wien University Library through its Open Access Funding Program.

ABSTRACT In the area of research on massive multiple-input multiple-output (MIMO), two assumptions on the wireless channel dominate channel modeling. Either, a rich scattering environment is assumed and the channel is modeled as i.i.d. Rayleigh fading, or, a line of sight (LOS) channel is assumed, enabling geometric channel modeling under a farfield assumption. However, either of these assumptions represents an extreme case that is unlikely to be observed in practice. While there is a variety of MIMO channel models in literature, most of them, and even very popular geometry based stochastic channel models, are not spatially consistent. This is especially problematic for technologies in which channel correlation of adjacent users is an important factor, such as massive MIMO. In this work, we introduce a simple but spatially consistent MIMO channel model based on multiple scattering theory. Our proposed channel model allows to adjust the Rician K factor by controlling the number and strength of scattering elements. This allows to perform spatially consistent simulations of wireless communications systems for a large range of scattering environments in between an i.i.d. Rayleigh fading assumption and pure LOS channels. A statistical analysis in terms of the Rician K factor for the introduced model is provided and verified by simulations. By comparison to other channel models, we show that non spatially consistent channel models lead to an underestimation of inter-user correlation and therefore to an overestimation of achievable sum rate.

INDEX TERMS Channel models, MIMO communications, massive MIMO.

I. INTRODUCTION

Massive MIMO promises to attain channel capacity in a multi-user MIMO scenario with simple linear precoding schemes. This optimal performance is attained under asymptotically favorable propagation conditions if the number of antennas at the base station (BS) tends to infinity [1]. The term *favorable propagation conditions* means that channel vectors are mutually orthogonal, that is, that the inter-user interference vanishes [2]. Massive MIMO supports dense scattering environments, that is, i.i.d. Rayleigh fading channels, as well as pure LOS scenarios [3]. While in the former case, channels become asymptotically orthogonal due to the law of large numbers, the latter case allows for the interpretation of forming increasingly sharp beams towards users [4].

For either of those extreme scenarios, simple channel models are at hand. Often, dense scattering environments are modeled by i.i.d. Rayleigh distributed channel coefficients. For pure LOS propagation, without any scattering objects within the propagation environment, channel coefficients are obtained by geometric models assuming planar wavefronts in a far field approximation. While in the former case, users are uncorrelated due to the independent generation of channel coefficients, in the latter case, channel correlation is implicitly given via geometry. Since massive MIMO is considered to be a multi-user MIMO system, the correlation of channels is critical for the communications system's performance [5]. There are several recent works considering the problem of

The associate editor coordinating the review of this article and approving it for publication was Kostas P. Peppas.

separating closely located users [6]–[8]. In order to investigate the impact of spatial correlation of co-located users, spatially consistent channel models are required. The property of spatial consistency in this context means that users in close proximity experience a higher correlation than well separated users on average.

In [9], the authors control the correlation between MIMO channels by varying the number and the angular spread of multi path components (MPCs) but do not employ a spatially consistent channel model. A user's channel correlation matrix is obtained by an exponential correlation model while there is no correlation assumed among users in [10]. Similarly in [11], a correlated MIMO channel is obtained by a matrix based correlation model. In [12], the LOS component is determined by geometry while the inter-user channel correlation matrix is obtained by the Gaussian local scattering model from [4].

Several channel models enable the analysis of MIMO wireless communications systems through link and system level simulations. The most popular models follow a geometric stochastic approach and consider clusters of scattering objects. MPCs within these clusters are then randomly generated according to specific large scale parameters (LSPs). Usually, LSPs are randomly drawn from a given distribution and the MPCs are then generated accordingly. This method is commonly applied within the Wireless World Initiative for New Radio (WINNER) channel models [13], [14], the 3rd Generation Partnership Project (3GPP) spatial channel model [15], [16], the 3GPP 3D channel model [17], [18] and the Quasi Deterministic Radio Channel Generator (QuaDRiGa) channel model [19]. Thereby, these models generate spatially correlated MIMO channels in terms of large scale fading. Even if the LSPs are generated spatially correlated, for example by 2D filtering as proposed in the QuaDRiGa channel model and the 3GPP 3D channel model, the resulting small scale fading is not spatially consistent for different users (users). In [20] and [21], authors put great effort into a modification of the 3GPP 3D model, in order to make it spatially consistent.

A different strategy is to generate a large number of MPCs first, and then to synthesize the LSPs from them. This method is adopted within the European Cooperation in Science and Technology (COST) 2100 channel model by introducing the concept of visibility regions for clusters [22]. The concept of visibility regions enables spatially consistent modeling of fading. However, this approach requires a proper choice of link cluster commonness in order to obtain a consistent model with multiple links [22]. In [23], for example, authors propose to augment the concept of visibility regions in the context of massive MIMO. As the COST 2100 channel model aims to reassemble specific scenarios that were observed in measurements, the set of supported scenarios is limited and the model does not allow to adjust the Rician K factor. For example, the implementation available in [24] offers an indoor hall scenario at 5 GHz and a semi-urban scenario at 300 MHz.

We propose a channel model that overcomes spatial consistency issues of stochastic geometric channel models, by considering geometric positions of scattering objects. This way, the introduced channel model becomes inherently spatially consistent. While this approach leads to a channel model that is spatially consistent on a large scale and on a small scale, we focus on small scale fading effects in our contribution. To develop an analytic statistical description of the channel model, based on positions of scattering objects distributed in space, we consider multiple scattering theory. This theory follows the simple idea that a radiated electromagnetic wave is re-radiated by each scattering element. We do not aim to restrict our model to certain specific scenarios but maintain flexibility to choose the density of the scattering environment to adjust the Rician K factor.

Multiple scattering theory was first employed in [25] and [26] to describe radio wave propagation through a random scattering environment. An extensive statistical analysis of multiple scattering propagation is provided in [27]. Based on this idea, a channel model based on stochastic propagation graphs is introduced in [28] and [29]. In these works, the authors consider multiple scattering events and derive closed form solutions for the case of an infinite number of scattering events [30].

A. CONTRIBUTION

We adopt the idea of multiple scattering theory from [25]. We assume a discrete set of scattering elements with isotropic re-radiation of electromagnetic waves. We furthermore consider a single scattering event for non-line of sight (NLOS) paths. By explicitly assigning spatial positions to scattering elements, transmit antennas and receive antennas, we obtain a spatially consistent MIMO channel model. The proposed channel model allows for adjustment of the Rician K factor, which enables investigation of wireless channels in between an i.i.d. Rayleigh fading channel and a pure LOS channel. We provide an analytic statistical analysis of our model in terms of the Rician K factor and verify the analysis by simulations. We show that non spatially consistent channel models overestimate the achievable sum rate as they underestimate the inter-user interference compared to the proposed spatially consistent model. As the complexity of the model scales only linearly with the number of antennas, the model is especially suited for simulation of massive MIMO systems with a large number of antennas.

B. NOTATION

We denote vectors by lowercase boldface symbols, such as $\mathbf{x}$, and matrices by uppercase boldface symbols, such as $\mathbf{X}$. The entry from the n^{th} row and the k^{th} column of matrix $\mathbf{X}$ is denoted by $[\mathbf{X}]_{n,k}$. We denote the Euclidean norm of vectors by $\|\cdot\|$ and the Frobenius norm by $\|\cdot\|_{\text{F}}$. The absolute value of a scalar as well as the cardinality of a set are denoted by $|\cdot|$. The transpose of a vector or matrix is denoted by $(\cdot)^{\text{T}}$ while the conjugate transpose of a vector or matrix is denoted by $(\cdot)^{\text{H}}$. The expectation of a random variable X is denoted

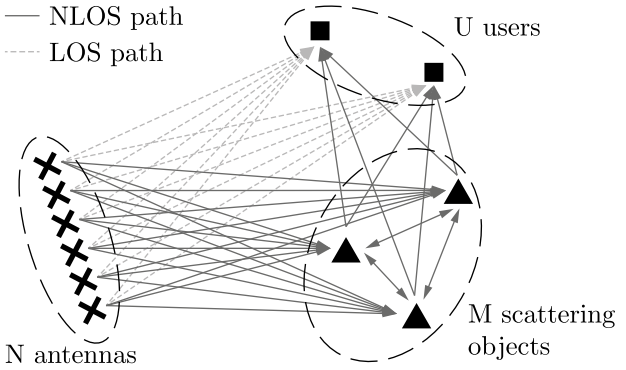

FIGURE 1. Nodes and propagation paths within the multiple scattering channel model. For this illustration, we chose $N = 6$, $M = 3$ and $U = 2$.

by $\mathbb{E}\{X\}$ while the variance of X is denoted by $\mathrm{var}\{X\}$. The trace of a matrix is denoted by $\mathrm{tr}(\cdot)$.

II. SPATIALLY CONSISTENT MIMO CHANNEL MODEL

In order to obtain a spatially consistent channel model, we consider a discrete set of scattering elements in free space. Assuming that a scattering event is described by an isotropic re-radiation of a wave corresponds to the idea of multiple scattering theory from [25] with an isotropic scattering kernel. As a simplification, we further assume that a scattering object cannot block propagation of electromagnetic waves. In line with this simplification, there is no self-scattering. This means that a scattering element re-radiates only a single wave rather than multiple ones. Applying a narrow band assumption, multiple rays that are scattered by a single scattering element cannot be distinguished. We cluster multiple scattered waves originating from one (or more than one) scattering element(s) and model them by a single scattering event. The cluster size is expressed via a clustering factor, describing the strength of the modeled scattering event. Therefore, a scattering element within the channel model may correspond to multiple scattering objects or scattered waves in a real-world scenario. The most important step to obtain a spatially consistent MIMO channel model is that each (transmit or receive) antenna, as well as each scattering object has an explicit location. While we employ a two dimensional space for all positions in this contribution, the proposed model is readily extended into three dimensions.

A complete statistical analysis of multiple scattering channel models is provided in [27]. There, the authors show that an L Rayleigh distribution, being the distribution of a product of L independent Rayleigh variables, is obtained for NLOS propagation with L scattering events. Since this distribution is only obtained in few special cases, as also shown in [27], we assume MPCs with a single bounce to be dominant and consider only a single scattering event in this work.

We assume N transmit antennas at positions $\mathbf{r}_n$ with $n \in \mathcal{T}$, where $\mathcal{T}$ denotes the set of transmit antenna indices with $|\mathcal{T}| = N$. There are U users with single antennas at positions $\mathbf{r}_u$ with $u \in \mathcal{R}$, where $\mathcal{R}$ denotes the set of user indices with $|\mathcal{R}| = U$. One may also interpret U as the number of receive antennas of a single user instead of a number of users with single antennas or any combination thereof. Further, we assume a discrete set of M scattering objects, located at positions $\mathbf{r}_p$ with $p \in \mathcal{S}$, where $\mathcal{S}$ denotes the set of scattering object indices with $|\mathcal{S}| = M$. The sets of node indices are unique in the sense that each index belongs to exactly one set, that is, $\mathcal{T} \cap \mathcal{R} = \mathcal{T} \cap \mathcal{S} = \mathcal{R} \cap \mathcal{S} = \emptyset$.

The channel is described by a MIMO channel matrix $\mathbf{H} \in \mathbb{C}^{U \times N}$ from N transmit antennas to U receive antennas or users, with transmit antenna $n \in \mathcal{T}$ at position $\mathbf{r}_n$ and receive antenna $u \in \mathcal{R}$ at position $\mathbf{r}_u$. The channel coefficient from transmit antenna n to receive antenna u is given by

$$[\mathbf{H}]_{u,n} = \alpha_{u,n} + \sum_{p \in \mathcal{S}} \beta_{u,p} \alpha_{p,n} \,, \tag{1}$$

where $\alpha_{u,n}$ describes propagation without any scattering, that is, the LOS path, and the sum term describes all propagation paths that include a scattering event.

We obtain the path coefficients α and β via simple wave propagation mechanisms assuming free space in between scattering objects. The path coefficients are given by

$$\alpha_{k,j} = \frac{\lambda}{4\pi \|\mathbf{r}_k - \mathbf{r}_j\|} e^{i\frac{2\pi}{\lambda}\|\mathbf{r}_k - \mathbf{r}_j\|} \,, \tag{2a}$$

$$\beta_{k,j} = \frac{\delta_j}{\sqrt{4\pi}\|\mathbf{r}_k - \mathbf{r}_j\|} e^{i\frac{2\pi}{\lambda}\|\mathbf{r}_k - \mathbf{r}_j\|} \,. \tag{2b}$$

Here, the coefficient $\alpha_{k,j}$ describes free space propagation from node j to node k. Coefficient $\beta_{k,j}$ describes the propagation from node j to node k, including a scattering event at node j (a scattering element) with the scattering coefficient δ_j. A scattering event at scattering object j is described by the complex valued scattering coefficient $\delta_j = \gamma_j e^{\phi_j}$ with the random phase $\phi_j \sim \mathcal{U}[0, 2\pi)$ and the clustering factor $\gamma_j = |\delta_j|$. The scattering phase is randomly drawn once per channel realization, in order to obtain a spatially consistent phase between transmitters and receivers. The clustering factor represents the strength of the scattering event and, therefore, reflects the physical size of the scattering object. We assume a fixed deterministic clustering factor in the sequel, that is $\gamma_j = \gamma, \forall j \in \mathcal{S}$. A detailed derivation of the path factors is provided in Appendix A.

Due to the presented choice of factors, the channel model, consisting of (1) and (2), includes path loss as well as small scale fading. However, we focus on spatial consistency of small scale fading in our contribution and do not apply a large scale fading model on top of free space LOS propagation. The number of transmit antennas, receive antennas and scattering objects is arbitrary and only limited by computational complexity. As the position of transmitters and receivers is free to choose, the introduced model is capable of modeling multi-user MIMO systems in a spatially consistent way with large arrays as well as distributed antenna systems.

The computation time to obtain channel coefficients according to the proposed channel model may be split into two parts. First, the generation of random positions for users

and scattering objects and second, the calculation of all channel coefficients according to (1) and (2). The asymptotic complexity for the generation of random positions scales linearly with the number of users and the number of scattering elements. Therefore, the asymptotic computational complexity of the first task is $\mathcal{O}(U) + \mathcal{O}(M)$. Computing all channel coefficients, that is the complexity of the second task, asymptotically scales with the number of scattering elements M. Since the channel coefficients have to be calculated for each combination of transmit antenna and receive antenna (or user), the asymptotic complexity is $\mathcal{O}(NUM)$, that is, linear in the number of transmit antennas, number of users and number of scattering objects. Therefore, the overall computational complexity of the proposed channel model is dominated by the latter part of calculating all channel coefficients.

III. STATISTICAL ANALYSIS

In this section, we investigate the distribution of channel coefficients for the proposed model and finally provide an expression for the K factor, depending on the number of scattering objects M and the clustering factor γ. Please note that although we define the K factor analogously to the Rician K factor, we do not make any assumption on the distribution of channel coefficients for the analysis provided in this section. We focus on the case of a fixed clustering factor γ in this work.

Inserting the scattering coefficients (2) and $\delta_p = \gamma e^{i\phi_p}$ into the model (1), we obtain

$$[\mathbf{H}]_{u,n} = \frac{\lambda}{4\pi \|\mathbf{r}_u - \mathbf{r}_n\|} e^{i\frac{2\pi}{\lambda}\|\mathbf{r}_u - \mathbf{r}_n\|} + \frac{\lambda\gamma}{(4\pi)^{\frac{3}{2}}} \sum_{p\in\mathcal{S}} u(\mathbf{r}_p), \quad (3)$$

with the sum term

$$u(\mathbf{r}_p) = \left(\|\mathbf{r}_u - \mathbf{r}_p\| \|\mathbf{r}_p - \mathbf{r}_n\|\right)^{-1} \times e^{i\left(\phi_p + \frac{2\pi}{\lambda}\left(\|\mathbf{r}_u - \mathbf{r}_p\| + \|\mathbf{r}_p - \mathbf{r}_n\|\right)\right)}. \quad (4)$$

From this relation, we observe that the BS, user and scattering object placement, that is, the scenario geometry, determines the channel statistics. The behavior of the sum in (3) is determined by the range of possible values of its sum terms (4). The absolute value of the sum term (4), depends on the BS-to-scattering object and the scattering object-to-user distances. Given a certain number of scattering objects, this sum might be dominated by a single value of large magnitude. This corresponds to the situation of a scattering object that is closely located to a transmit antenna or receive antenna. To bound the sum term's absolute value, we consider a minimum distance $d_S > 0$ between any transmit and any receive antenna to any scattering object, that is

$$\|\mathbf{r}_k - \mathbf{r}_m\| \geq d_S \quad \forall k \in \mathcal{T} \cup \mathcal{R}, \ \forall m \in \mathcal{S}. \quad (5)$$

This condition is straight forward to fulfill in any simulation scenario, by introducing an empty region with radius d_S around all BS and user antennas in which no scattering object is placed. The condition (5) guarantees the existance and boundedness of (3). Bounds on the magnitude of (4) are discussed in more detail in Appendix B.

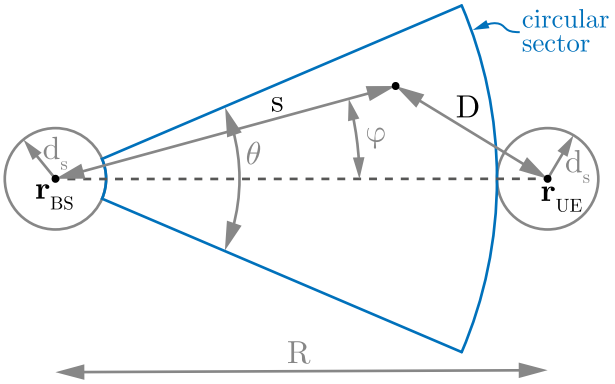

FIGURE 2. Circular sector geometry considered for calculation of the channel coefficient variance.

A. PHASE DISTRIBUTION OF SUM TERMS

To investigate the phase of the sum terms $u(\mathbf{r}_p)$, we introduce the following lemma.

Lemma 1 (Distribution of Modulo Sum): Let X be a random variable, uniformly distributed in the interval $[0, a)$ with $a > 0$ and Y be a random variable independent of X. Then, $(X + Y) \bmod a$ is again uniformly distributed in $[0, a)$, independent of the distribution of Y.

Defining the argument of a complex number $z \in \mathbb{C}$ as $\text{Arg}\left(|z|e^{i\phi}\right) = \phi \bmod 2\pi$, the phase of the sum terms is given by

$$\text{Arg}\left(u(\mathbf{r}_p)\right) = \phi_p + \frac{2\pi}{\lambda}\left(\|\mathbf{r}_u - \mathbf{r}_p\| + \|\mathbf{r}_p - \mathbf{r}_n\|\right) \bmod 2\pi. \quad (6)$$

As the scattering phase ϕ_p is uniformly distributed within $[0, 2\pi)$ and independent of the scattering object and user placement, invoking Lemma 1 we obtain

$$\text{Arg}\left(u(\mathbf{r}_p)\right) \sim \mathcal{U}[0, 2\pi). \quad (7)$$

Therefore, the sum term has a uniformly distributed phase, independent of the scattering object placement and scenario geometry.

B. VARIANCE OF SUM TERMS

In order to find an expression for the Rician K factor for the proposed channel model, the variance of the sum terms $u(\mathbf{r}_p)$ is required. As shown in the previous section, the phase of $u(\mathbf{r}_p)$ is uniformly distributed, if the scattering phase is uniformly distributed within $[0, 2\pi)$. Further, the magnitude distribution and the phase distribution of $u(\mathbf{r}_p)$ are independent. Therefore, $u(\mathbf{r}_p)$ is complex circularly distributed around zero and therefore has zero mean, that is, $\mathbb{E}\left\{u(\mathbf{r}_p)\right\} = 0$.

To find an expression for the variance $\omega^2 = \text{var}\left\{u(\mathbf{r}_p)\right\}$, we consider the geometry shown in Fig. 2. Here, we assume that the user is located at the middle of the sector, that is, at an angle of $\varphi = 0$. When considering a distribution of users with

a random angle, this is an approximation assuming that the maximum user angle is smaller than the sector angle.

Considering (4) in terms of the geometry shown in Fig. 2, we identify the transmitter-to-scattering object distance $\|\mathbf{r}_p - \mathbf{r}_n\|$ to be s and the scattering object-to-receiver distance $\|\mathbf{r}_u - \mathbf{r}_p\|$ to be D.

We consider a random variable transformation to obtain an expression for the variance ω^2. A two dimensional uniform distribution of scattering object positions within the circular sector is equivalent to a uniform distribution of the angle φ and a triangular distribution of the distance to the BS s. Their probability density functions (PDFs) are given by

$$f_\varphi(\varphi) = \begin{cases} \frac{1}{\theta} & \text{for } -\frac{\theta}{2} \le \varphi \le \frac{\theta}{2} \\ 0 & \text{otherwise} \end{cases}, \tag{8}$$

and

$$f_s(s) = \begin{cases} \frac{2}{s_{\max}^2 - s_{\min}^2} s & \text{for } s_{\min} \le s \le s_{\max} \\ 0 & \text{otherwise} \end{cases}, \tag{9}$$

where the minimum value of s is given by $s_{\min} = d_S$ and the maximum value of s is given by $s_{\max} = R - d_S$. Since φ and s are independent, their joint PDF is given by $f_{s,\varphi}(s, \varphi) = f_s(s) f_\varphi(\varphi)$. Considering a scattering object location with distance s from the transmitter at angle φ and distance D to the receiver and applying the law of cosines, a random variable transform of the form

$$|u|^2 = Y = g(s, \varphi) = \left(s^2 \left(R^2 + s^2 - 2Rs\cos(\varphi)\right)\right)^{-1} \tag{10}$$

is performed. Applying the random variable transform to calculate the variance of u, we obtain

$$\begin{aligned} \omega^2 &= \operatorname{var}\{u\} = \mathbb{E}\left\{|u|^2\right\} = \mathbb{E}\{Y\} \\ &= \int Y f_{\mathcal{Y}}(Y) dY \\ &= \int_{-\frac{\theta}{2}}^{\frac{\theta}{2}} \int_{s_{\min}}^{s_{\max}} g(s, \varphi) f_{s,\varphi}(s, \varphi)\, ds\, d\varphi \\ &= \frac{8}{\theta\left(s_{\max}^2 - s_{\min}^2\right)} \\ &\quad \times \int_{s_{\min}}^{s_{\max}} \frac{1}{s(R-s)} \arctan\left(\frac{R+s}{R-s} \tan\left(\frac{\theta}{4}\right)\right) ds, \end{aligned} \tag{11}$$

where $\mathbb{E}\{u(\mathbf{r})\} = 0$ was employed.

C. K FACTOR ANALYSIS

Assuming random and independent user positions as well as random and independent scattering object positions, the sum terms (4) from (3) have zero mean and are independent. Invoking the central limit theorem, the sum is approximately Gaussian distributed as long as M is sufficiently large. We denote the resulting complex symmetric Gaussian random variable by X and can therefore approximate the channel coefficient as

$$[\mathbf{H}]_{u,n} \approx \left[\widetilde{\mathbf{H}}\right]_{u,n} = \alpha_{u,n} + \frac{\lambda\gamma}{(4\pi)^{\frac{3}{2}}} X, \tag{12}$$

where $X \sim \mathcal{CN}\left(0, M\omega^2\right)$. Assuming a fixed but arbitrary position $\mathbf{r}_u$, corresponding to the BS antenna position, without loss of generality, $\alpha_{u,n}$ is deterministic for a given user to BS distance $R = \|\mathbf{r}_u - \mathbf{r}_n\|$, even if the user's antenna position $\mathbf{r}_n$ is random. Therefore, the approximated channel coefficients are distributed as $\left[\widetilde{\mathbf{H}}\right]_{u,n} \sim \mathcal{CN}\left(\alpha_{u,n}, M\,(\omega\gamma)^2 \frac{\lambda^2}{(4\pi)^3}\right)$. While the number of scattering elements M required for a good approximation (12) depends on the minimum distance d_S, a few tens of scattering objects already lead to a good approximation for a few meters of d_S.

Let us consider the K factor of the absolute value of the channel coefficients $\left|\left[\widetilde{\mathbf{H}}\right]_{u,n}\right|$ as the ratio of power in the specular (LOS) component to the power of the MPCs

$$K = \frac{|\nu|^2}{\sigma^2}, \tag{13}$$

analogous to the notion of a Rician K factor. Here, $\nu = \mathbb{E}\left\{\left[\widetilde{\mathbf{H}}\right]_{u,n}\right\}$ is the mean, contributed through the LOS component, and $\sigma^2 = \operatorname{var}\left\{\left[\widetilde{\mathbf{H}}\right]_{u,n}\right\}$ is the variance .

Considering (12) we find

$$|\nu|^2 = |\alpha_{u,n}|^2 = \left(\frac{\lambda}{4\pi R}\right)^2, \tag{14}$$

$$\sigma^2 = M\,(\gamma\omega)^2 \frac{\lambda^2}{(4\pi)^3}, \tag{15}$$

which leads to a K factor of

$$K = \frac{4\pi}{M\,(\gamma\omega R)^2}. \tag{16}$$

While it is not surprising that the K factor depends on the user to BS distance via Friis' formula, (16) further reveals the dependence upon the number of scattering objects M and the clustering factor γ. It is intuitive that the K factor decreases with an increasing number of scattering objects as well as with an increasing clustering factor, as this renders scattered paths dominant compared to the LOS path. While the clustering factor γ is a constant factor within the sum terms $u(\mathbf{r}_p)$, and therefore appears squared in their variance, the factor ω^2 is dependent on the scenario geometry. As previously mentioned, the variance is increased for small antenna to scattering object and inter-scattering object distances d_S.

IV. SIMULATION RESULTS

In this section we present and discuss simulation results obtained with the proposed channel model. Firstly, we demonstrate that the statistical model analysis from Section III is correct and the introduced approximation is valid. Secondly, to verify the introduced model, we compare simulation results in terms of spatial correlation to a simple *Rice* channel model and the 3GPP 3D channel model from [17]. The simulation scenario employed for the proposed channel model is as shown in Fig. 3. The scattering objects are uniformly distributed within a circular sector of 120° with an inner radius of 10 m and an outer radius of 50 m. The users have a single antenna each and are placed

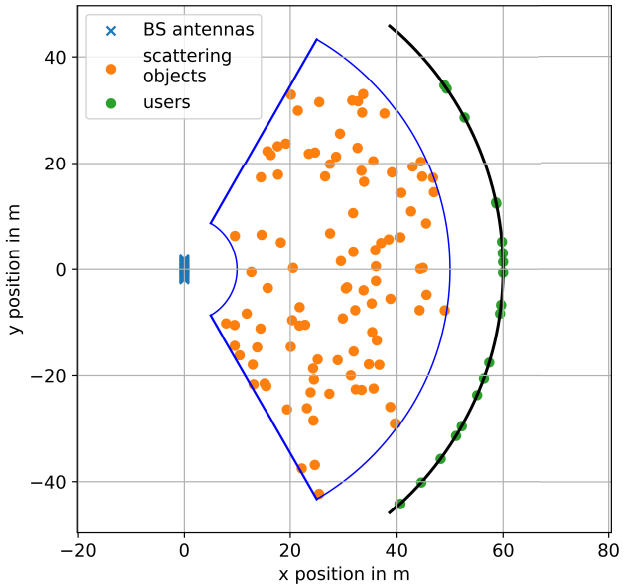

FIGURE 3. Simulation scenario geometry. The circular sector is outlined in blue. Possible user positions are indicated in black. User positions and scattering object positions in this figure are taken form a single realization. For the purpose of illustration we chose $M = 100$ scattering objects, $N = 64$ transmit antennas and $U = 20$ users.

at a constant distance of 60 m from the BS with a uniformly distributed polar angle of $[-50, 50]$ degrees. With this setup, a minimum distance between users and scattering objects as well as between BSs and scattering objects is automatically ensured. The BS is equipped with a uniform linear array (ULA) of $N = 64$ antennas along the y-axis with the array center at the origin. The elements of the ULA are spaced by $\lambda/2$ at a carrier frequency of 2.5 GHz. All antenna elements, user antennas and BS antennas, are omnidirectional.

A. AMPLITUDE DISTRIBUTION

In order to verify the statistical description of the proposed channel model in terms of a K factor, we perform simulations of channel amplitude distributions in this section. Simulations with 1 000 random realizations of user positions and scattering object positions are performed. We employ $M = 800$ scattering objects within the previously described simulation scenario. Results in terms of cumulative distribution functions of the channel coefficient magnitude are shown in Fig. 4 for different clustering factors γ. For this simulation result, the mean channel power was normalized to one. The maximum likelihood (ML) distribution fits for a Rice as well as for a Nakagami-m distribution are provided. For the Rice distribution, the Rician K factor $\hat{K}_{\mathrm{ML}}$ is obtained by ML estimation and for the Nakagami-m distribution the shape factor $\hat{m}_{\mathrm{ML}}$ is ML estimated. The corresponding values for both parameters are provided in Fig. 4 as well. Both distributions, the Rician and the Nakagami-m, show a good match with the simulation data.

A Rician fading amplitude distribution of channel coefficients is obtained by assuming the presence of one

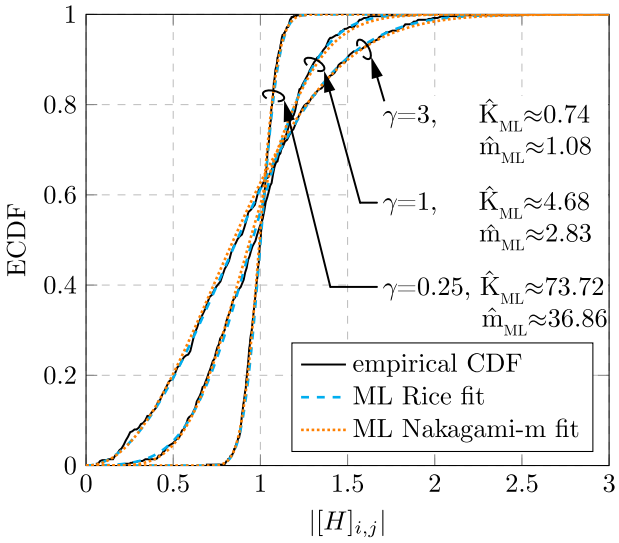

FIGURE 4. ML fit of Rice distribution to simulated channel coefficient's magnitude with $M = 800$ scattering objects.

specular component and many diffuse multipath components. A Nakagami-m distribution [31] of amplitudes is obtained through maximum ratio combining of m Rayleigh fading channel coefficients. While a Nakagami-m distribution with $m = 1$ is equivalent to a Rayleigh distribution, a Rician distribution is approximated by the Nakagami-m distribution when choosing the shape parameter according to [31]

$$m = \frac{(K+1)^2}{2K+1}. \tag{17}$$

Please note that the Rician K factor and the Nakagami-m shape parameter m provided in Fig. 4, which are obtained independently by ML estimation, approximately fulfill relation (17).

From the results shown in Fig. 4 we observe that both, the Rician and the Nakagami-m distribution, provide a good fit with the data obtained by simulation. Therefore, the statical analysis provided in Section III can also be performed in terms of the Nakagami-m shape parameter

$$m = \frac{\left(\mathbb{E}\left\{\left|[\widetilde{\mathbf{H}}]_{u,n}\right|^2\right\}\right)^2}{\mathrm{var}\left\{\left|[\widetilde{\mathbf{H}}]_{u,n}\right|^2\right\}}. \tag{18}$$

However, due to the geometric interpretability of Rician fading, which suites our channel model very well, we performed the statistical description in terms of a K factor in Section III. Since the amplitude distribution obtained through simulation fits a Rician one, we indeed identify the introduced K factor to be the Rician K factor.

Employing the same simulation setup, the derived relation for the Rician K factor (16) is verified. Given the geometry, the variance ω^2 is calculated through (11). Simulation results for K over the number of scattering objects M are shown in Fig. 5. Again, 1 000 random realizations were performed. In both cases, the calculated Rician K factor is compared to its

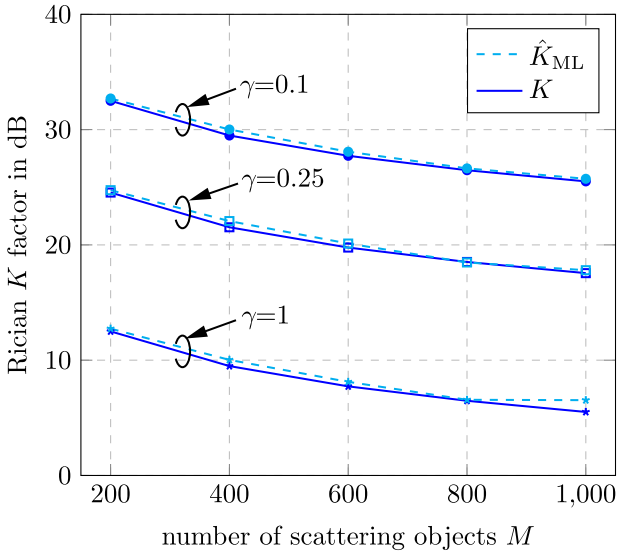

FIGURE 5. Comparison of the analytically predicted Rician K factor K and the ML estimated Rician K factor $\hat{K}_{\mathrm{ML}}$.

ML estimate, which is denoted by $\hat{K}_{\mathrm{ML}}$. Please recall that (11) is obtained as an approximation, where we assume to user to be located at the middle of the sector, that is, at $\varphi = 0$. Although simulations performed here employ a uniform user distribution within $[-50°, 50°]$, the predicted K factor and the ML estimated K factor show a good fit. This shows the validity of the approximation within the derivation of (16).

B. SPATIAL CONSISTENCY

To demonstrate the key feature of our proposed channel model, which is spatial consistency, we perform simulations with the same sector geometry as shown in Fig. 3. To investigate the spatial correlation, we again consider a random placement of scattering objects but a deterministic placement of $U = 2$ users. While both users are at distance $R = 60\,\mathrm{m}$ from the BS, the first user is placed at an angle of $\varphi/2$ and the second user is placed at an angle of $-\varphi/2$, relative to the array broadside direction. In this setup, the MIMO channel matrix consists of the users' channel vectors $\mathbf{h}_u \in \mathbb{C}^{N\times 1}$ containing channel coefficients from N antennas to user u, i.e., $\mathbf{H} = (\mathbf{h}_1, \mathbf{h}_2)^{\mathrm{T}}$.

As a comparison, we consider a *Rice* MIMO channel model of the form

$$\mathbf{H}_{\mathrm{Rice}} = \sqrt{\frac{K}{1+K}}\mathbf{H}_{\mathrm{LOS}} + \sqrt{\frac{1}{1+K}}\mathbf{H}_{\mathrm{iid}} \in \mathbb{C}^{U\times N} \,. \quad (19)$$

The i.i.d. Rayleigh fading channel matrix $\mathbf{H}_{\mathrm{iid}}$ contains Gaussian distributed channel coefficients, that is, $\left[\mathbf{H}_{\mathrm{iid}}\right]_{u,n} \sim \mathcal{CN}(0,1)$. The columns of $\mathbf{H}_{\mathrm{LOS}}$ are given by the LOS far field channel vectors to all users. Assuming a ULA with antenna spacing d, the LOS channel vector for user u is given by

$$\mathbf{h}_{\mathrm{LOS},u} = \left(e^{-i\frac{N}{2}\frac{2\pi}{\lambda}d\sin(\varphi_u)}, \ldots, e^{i\frac{N}{2}\frac{2\pi}{\lambda}d\sin(\varphi_u)}\right)^{\mathrm{T}} , \quad (20)$$

where φ_u is the angular position of user u.

As a metric for spatial correlation of users' channel vectors, we consider the normalized inner product

$$\rho(\varphi) = \mathbb{E}\left\{\frac{|\mathbf{h}_1^{\mathrm{H}}\mathbf{h}_2|}{\|\mathbf{h}_1\|\|\mathbf{h}_2\|}\right\} , \quad (21)$$

similar as done in [32]. Considering maximum ratio transmission precoding in the case of two users, ρ^2 is the inter-user interference power. For two identical channel vectors $\rho = 1$, while two orthogonal channel vectors yield $\rho = 0$. We identify two criterions in terms of the spatial correlation metric $\rho(\varphi)$ for a spatially consistent channel model:

1) Users at the same position must experience the same channel and therefore a correlation of one:

$$\rho(0) = 1 \,. \quad (22a)$$

2) For a bounded variation in position φ, the change in correlation must be bounded as well, that is, the correlation function must be Lipschitz continuous:

$$\rho(\varphi_1) - \rho(\varphi_2) \leq L\,(\varphi_1 - \varphi_2) \,, \quad (22b)$$

for a Lipschitz constant $L \geq 0$ and two arbitrary user positions $\varphi_1, \varphi_2 \in [0, 2\pi)$.

Simulation results in terms of $\rho(\varphi)$ over the angle between the two users φ are shown in Fig. 6. While results shown in Fig. 6a and Fig. 6b are obtained with the same parameters, the latter is considered as a detail view of the former with respect to small angles between users. Results for the normalized inner product ρ are provided for four different Rician K factors of $K = -6\,\mathrm{dB}, 0\,\mathrm{dB}, 6\,\mathrm{dB}, 17\,\mathrm{dB}$ for the proposed channel model and the *Rice* channel model. For our proposed channel model, these K factor values are obtained with $M = 800$ scattering objects and clustering factors of $\gamma \approx 4.24, 2.14, 1.08, 0.28$. The two extreme cases, a pure *LOS* channel, that is, $K \to \infty$, and an i.i.d. Rayleigh fading channel, that is $K \to 0$, are provided as a reference.

From Fig. 6a we observe that the pure LOS channel and the proposed channel model are spatially consistent, as they fulfill criterion (22a). The proposed channel model achieves a very good fit with the *Rice* channel model (19) of the same Rician K factor, except for the region around $\varphi = 0$. To investigate this region of small inter-user angles further, Fig. 6b is provided. Here, we observe that the spatial correlation of the proposed channel model is indeed spatially consistent, as its smooth behavior also fulfills criterion (22b).

All other compared channel models are not spatially consistent as they violate criterion (22a). Since we generate the i.i.d. Rayleigh fading channel by drawing channel coefficients from a complex Gaussian distribution without any dependence on the user position, two users at the same position experience different channels. However, even if the generation of channel coefficients was changed, such that two users at the same position are assigned identical channel coefficients, still does not render the channel model spatially consistent. While this leads to $\rho(0) = 1$ and therefore fulfills

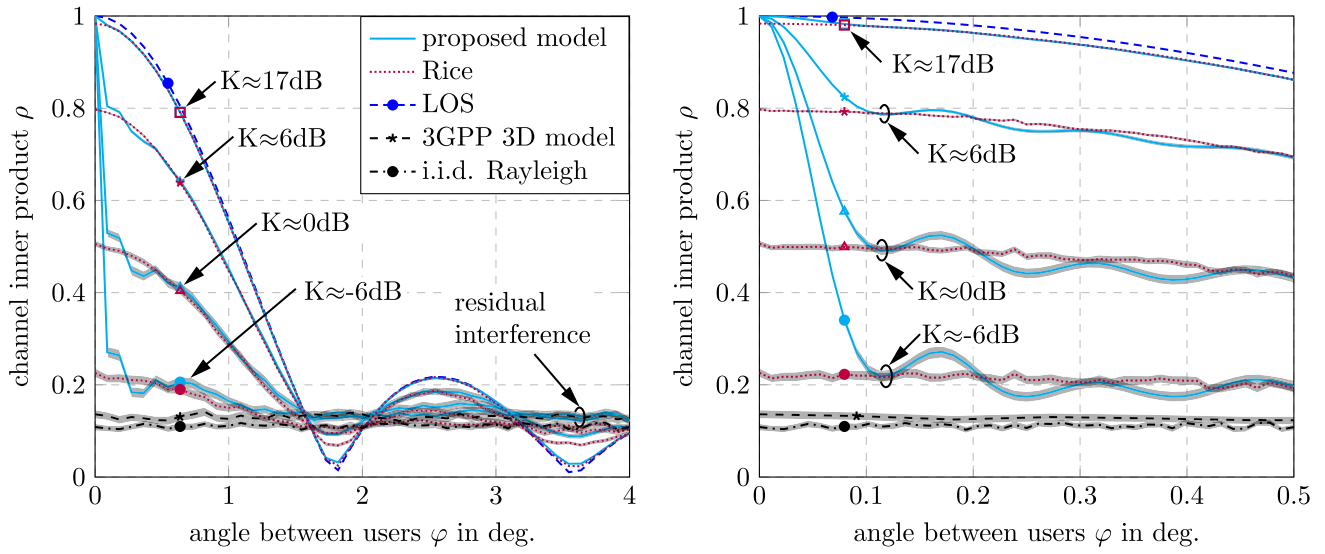

(a) Wide angular range.

(b) Narrow angular range.

FIGURE 6. Normalized inner product over inter-user distance for (a) a wide angular range and (b) a narrow angular range. The proposed channel model as well as the pure LOS channel are spatially consistent. The 95% confidence regions obtained by bootstrapping are highlighted in gray.

the first criterion, this alternate generation of channel coefficients leads to a violation of criterion (22b) as the correlation suddenly drops for user distances larger than zero.

As a comparison, the spatial correlation obtained with the 3GPP 3D channel model with the same scenario geometry as previously described is also provided in Fig. 6. For this channel model, we assume an urban micro cell scenario with 12 clusters and 20 rays per cluster. To obtain a fair comparison, we exclude shadow fading effects of the 3GPP 3D channel model for our simulation. Since the small scale fading within this channel model is generated uncorrelated for different users, the obtained spatial correlation shows no spatial consistency.

Another important observation from these simulation results is the *residual interference* at comparably high inter-user angles, as indicated in Fig. 6a. The spatial correlation remains higher than the one obtained with an i.i.d. Rayleigh fading assumption, even for high values of φ. This residual correlation originates from the location of scattering objects on only one side of the user. The i.i.d. Rayleigh fading case is attained with a spatial channel model only, if there is a ring of scattering elements placed around the user. Although we assume a pure NLOS channel for the 3GPP 3D channel model, the spatial correlation is also higher than the i.i.d. Rayleigh fading channel. This again stresses that the i.i.d. Rayleigh fading assumption is only achieved by artificial scenario geometries with spatial channel models.

C. ACHIEVABLE SPECTRAL EFFICIENCY

In this section we consider the effects of spatial consistency on the achievable rate of a massive MIMO communications system. We consider a multi-user MIMO downlink system. The vector of received signals for U users is given by

$$\mathbf{y} = \mathbf{H}^{\mathrm{H}}\mathbf{F}\mathbf{x} + \mathbf{w} \in \mathbb{C}^{U\times 1}\,, \tag{23}$$

where $\mathbf{x} \in \mathbb{C}^{U\times 1}$ is the vector of random transmit symbols, $\mathbf{F}$ is the precoding matrix and $\mathbf{w}$ is additive white Gaussian noise, that is, $\mathbf{w} \sim \mathcal{CN}\left(\mathbf{0}, \sigma_w^2\mathbf{I}_U\right)$. We employ independent transmit symbols of unit power, that is, $\mathbb{E}\left\{\mathbf{x}\mathbf{x}^{\mathrm{H}}\right\} = \mathbf{I}_U$. The channel matrix $\mathbf{H}$ is given by $\mathbf{H} = (\mathbf{h}_1, \ldots, \mathbf{h}_U)$, where column vectors are the channel vectors for each user. A user's channel vector is given by $\mathbf{h}_k = \sqrt{\eta_k}\tilde{\mathbf{h}}_k$ for $k \in \{1, \ldots, U\}$ where $\eta_k > 0$ denotes the large scale fading coefficient of user k and $\tilde{\mathbf{h}}_k$ describes the small scale fading with $\left\|\tilde{\mathbf{h}}_k\right\| = 1\ \forall k$. Since the transmit symbols are of unit power, a sum power constraint of the form $\mathbb{E}\left\{\|\mathbf{F}\mathbf{x}\|_2^2\right\} \leq P_T$ leads to the requirement $\|\mathbf{F}\|_{\mathrm{F}}^2 \leq P_T$. We consider a zero forcing (ZF) precoder given by

$$\mathbf{F}_{\mathrm{ZF}} = \frac{\sqrt{P_T}}{\sqrt{\mathrm{tr}\left(\left(\mathbf{H}^{\mathrm{H}}\mathbf{H}\right)^{-1}\right)}}\,\mathbf{H}\left(\mathbf{H}^{\mathrm{H}}\mathbf{H}\right)^{-1}\,, \tag{24}$$

fulfilling the power constraint. Therefore, the signal to noise ratio (SNR) of user k is

$$\mathrm{SNR}_k = \frac{P_T}{\sigma_w^2\,\mathrm{tr}\left(\left(\mathbf{H}^{\mathrm{H}}\mathbf{H}\right)^{-1}\right)}\,. \tag{25}$$

The achievable downlink sum spectral efficiency (SE) is obtained as

$$R_{\mathrm{sum}} = \sum_{k=1}^{U}\log_2\left(1+\mathrm{SNR}_k\right)\,. \tag{26}$$

Again, we perform simulations with a scenario geometry as shown in Fig. 3 and previously described in Section IV.

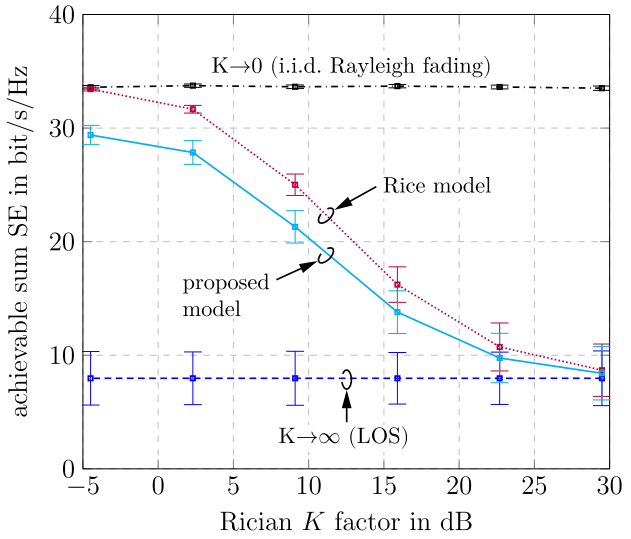

FIGURE 7. Achievable sum SE with ZF precoding with 95% confidence intervals obtained by bootstrapping.

We assume a downlink transmission to $U = 20$ users, which are placed at a distance of $R = 60\,\text{m}$ with uniformly distributed angles φ_u within $[-50°, 50°]$. For a typical massive MIMO downlink scenario, we choose $\sigma_w^2 = 1$ and $P_T = 1/\eta$ to obtain an SNR of 0 dB in the interference free case. Please note that we assume $\eta_k = \eta\ \forall k$, which is automatically achieved in our simulation scenario due to the user placement. Simulation results for the achievable downlink sum SE over the Rician K factor are shown in Fig. 7.

Together with the results for the *Rice* channel model according to (19) and the proposed channel model, we provide bounds for $K \to \infty$ (LOS) and $K \to 0$ (i.i.d. Rayleigh fading). Due to the ZF precoding, the achievable rate is significantly higher for an i.i.d. Rayleigh fading channel compared to the LOS channel assumption. This shows that there is a significant amount of inter-user correlation in the LOS case, since the randomly distributed users cannot be separated with the $N = 64$ antenna ULA. Therefore, a significant loss in signal power is experienced with ZF precoding in the high K factor regime.

Necessarily, through the definition of the *Rice* channel model, its achievable rate converges to the same rate as the i.i.d. Rayleigh fading channel model for low K factors and to the same rate as the LOS channel for high K factors. While the proposed channel model has a similar trend over the Rician K factor, it shows a gap to the *Rice* channel model for low K factors. This behavior shows the importance of spatial consistency for multi-user MIMO applications. As explained in Section IV-B, the proposed model yields high correlation for very closely spaced users, c.f., Fig. 6, as well as correlation that is higher compared to the i.i.d. Rayleigh fading assumption also at larger inter-user distances. Although the difference in spatial correlation between the proposed and the *Rice* channel model seems to be limited, c.f. Fig. 6, the impact on the achievable SE is significant. To investigate the impact of user channel correlation on the SE, we derive an upper bound on the SNR in Appendix C, which is given by

$$\text{SNR} \leq \frac{\eta P_T}{\sigma_w^2} \left(1 - \max_{\substack{i,j \\ i \neq j}} \left| \tilde{\mathbf{h}}_i^{\text{H}} \tilde{\mathbf{h}}_j \right| \right) . \tag{27}$$

Since the users are placed with equal distance to the BS, we assumed the same large scale fading coefficient η, that is path loss, for all users for the derivation of this bound. Please note that since the vectors $\tilde{\mathbf{h}}_k$ are normalized $0 \leq \left| \tilde{\mathbf{h}}_i^{\text{H}} \tilde{\mathbf{h}}_j \right| \leq 1$ for $i \neq j$ and $i, j \in \{1, \ldots, U\}$. From (27) we observe that the SNR depends on the inner product of channel vectors, such as the previously introduced correlation measure (21). The upper bound on the SNR is decreasing with increasing correlation, showing the negative impact of user correlation on the achievable SE with ZF precoding. Moreover, the bound is given by the maximum magnitude of channel vectors between any two users. This shows that the sum SE is decreased if any two users are highly correlated. In the limit, we obtain SNR $\to 0$ if there are any two users i and j with $\left| \tilde{\mathbf{h}}_i^{\text{H}} \tilde{\mathbf{h}}_j \right| \to 1$.

Since for increasing Rician K factors, the proposed model and the *Rice* channel model both converge to the spatially consistent LOS channel, the gap in achievable rate is decreasing with increasing K factor. The gap in achievable rate occurs, since the not spatially consistent i.i.d. Rayleigh fading model underestimates the amount of spatial correlation between users. Please note that the LOS is always present in our proposed channel model and does not vanish for very low values of K.

V. CONCLUSION

In this work, we introduce a channel model based on multiple scattering theory. By employing simple propagation mechanisms, we obtain a low complexity MIMO channel model. We consider only single scattering events for NLOS paths. Adjusting the number and strength of scattering events allows to adjust the Rician K factor of the model. This allows to simulate propagation environments in between rich scattering and pure LOS channels. We provide a statistical description for the Rician K factor of the proposed model and verify it by simulation. Investigating the model's spatial correlation properties, we show that the proposed channel model is indeed spatially consistent while the simplified assumption of i.i.d. Rayleigh fading and the 3GPP 3D channel model are not. Non spatially consistent channel models lead to an underestimation of spatial correlation among users and therefore to an overestimation of achievable sum rate. This underlines the importance of spatially consistent channel models for investigation of multi-user MIMO systems such as massive MIMO.

APPENDIX A
DERIVATION OF SCATTERING COEFFICIENTS

In the channel model (1), $\alpha_{k,j}$ describes propagation on a direct path from transmit antenna position $\mathbf{r}_j$ to positions $\mathbf{r}_k$,

where either a receive antenna or a scattering object is located at $\mathbf{r}_k$. Further, $\beta_{k,j}$ describes the propagation from position $\mathbf{r}_j$ to positions $\mathbf{r}_k$ including a scattering event at position $\mathbf{r}_j$ where either a receive antenna or an other scattering object is located at $\mathbf{r}_k$. In order to find physically meaningful expressions for the factors α and β, we consider a bi-static radar. In this setup, a transmitter emits a wave that is scattered at a target and received by a receiver, which is not co-located with the transmitter. The bi-static radar equation [33] is given by

$$\frac{P_r}{P_t} = \frac{G_t}{4\pi d_1^2}\,\gamma^2\,\frac{A_{\mathrm{r,eff}}}{4\pi d_2^2}\,, \tag{28}$$

with the distance d_1 between the transmitter and the target and the distance d_2 between the target and the receiver. Equation (28) describes the ratio between the received power P_r by an antenna with effective area A_{eff} and the transmitted power P_t from a transmit antenna with gain G_t. Here, γ^2 is the radar cross section of the target. Next, we insert the relation between the effective antenna aperture and antenna gain

$$A_{\mathrm{r,eff}} = \frac{\lambda^2}{4\pi} G_r\,, \tag{29}$$

and assume $G_r = G_t = 1$. Since the power is proportional to the square of the electrical field strength E, we obtain a ratio between the received and the transmitted field strength, including one scattering event as

$$\frac{E_r}{E_t} = \underbrace{\frac{1}{\sqrt{4\pi}d_1} e^{\frac{2\pi}{\lambda}d_1}}_{\text{transmitter to scatt.}} \underbrace{\gamma e^{i\phi_p}}_{\substack{\text{scattering}\\ \text{event}}} \underbrace{\frac{\lambda}{4\pi d_2} e^{\frac{2\pi}{\lambda}d_2}}_{\text{scatt. to receiver}}\,. \tag{30}$$

The phase of (30) is determined by free space propagation from the transmitter to the scattering object, free space propagation from the target to the receiver and a random scattering phase ϕ_p.

Taking this idea further, to the case of multiple scattering events and considering the structure of the model (1), we obtain the path coefficients

$$\alpha_{k,j} = \frac{\lambda}{4\pi\|\mathbf{r}_k - \mathbf{r}_j\|} e^{i\frac{2\pi}{\lambda}\|\mathbf{r}_k - \mathbf{r}_j\|}\,, \tag{31a}$$

$$\beta_{k,j} = \frac{\delta_j}{\sqrt{4\pi}\|\mathbf{r}_k - \mathbf{r}_j\|} e^{i\frac{2\pi}{\lambda}\|\mathbf{r}_k - \mathbf{r}_j\|}\,. \tag{31b}$$

The magnitude of parameter $\alpha_{k,j}$ corresponds to Friis' formula for free space propagation between positions $\mathbf{r}_j$ and $\mathbf{r}_k$. The factor $\beta_{k,j}$ includes a scattering event at scattering object j via the scattering coefficient $\delta_j = \gamma_j e^{\phi_j}$ with clustering factor γ_j and the random phase ϕ_j.

APPENDIX B
BOUNDS ON THE MAGNITUDE OF SUM TERMS

In this section we consider bounds on the magnitude of the sum term (4) and provide bounds for a circular sector geometry. For readability, we consider a single transmit antenna and a single receive antenna and denote $\mathbf{r}_n$ as the BS position $\mathbf{r}_{\mathrm{BS}}$, $\mathbf{r}_u$ as the user position $\mathbf{r}_{\mathrm{UE}}$ and $\mathbf{r}_p$ as the scattering object position $\mathbf{r}_{\mathrm{S}}$ in the sequel. In order to bound $|u(\mathbf{r}_{\mathrm{S}})|$ from above and therefore guarantee boundedness of channel coefficients, the distances $\|\mathbf{r}_{\mathrm{BS}} - \mathbf{r}_{\mathrm{S}}\|$ and $\|\mathbf{r}_{\mathrm{S}} - \mathbf{r}_{\mathrm{UE}}\|$ must not become arbitrarily small. We consider a minimum distance between a scattering object and any antenna, belonging to either a user or the BS, as d_{S}. To bound the sum terms, the minimum and maximum product of user-to-scattering object and scattering object-to-BS distance is decisive. We obtain the following problem to determine the minimum product of distances as

$$\begin{aligned}\xi_{\min} = \min_{\mathbf{r}_{\mathrm{S}}}\ & \|\mathbf{r}_{\mathrm{BS}} - \mathbf{r}_{\mathrm{S}}\|\,\|\mathbf{r}_{\mathrm{UE}} - \mathbf{r}_{\mathrm{S}}\| \\ \text{subject to } & \|\mathbf{r}_{\mathrm{BS}} - \mathbf{r}_{\mathrm{S}}\| \geq d_{\mathrm{S}} \\ & \|\mathbf{r}_{\mathrm{UE}} - \mathbf{r}_{\mathrm{S}}\| \geq d_{\mathrm{S}}\end{aligned} \tag{32}$$

where the constraints correspond to the minimum distance between BS and scattering object and between user and scattering object. Similarly, changing (32) to a maximization problem with the same cost function and constraints leads to the solution $\xi_{\max}$. These extrema allow us to state lower and upper bounds on the absolute value of the sum terms $u(\mathbf{r}_{\mathrm{S}})$ as

$$\frac{1}{\xi_{\max}} \leq |u(\mathbf{r}_{\mathrm{S}})| \leq \frac{1}{\xi_{\min}}\,. \tag{33}$$

From the upper bound, we conclude that it is necessary and sufficient for boundedness of (3) that there exists a minimum distance $d_{\mathrm{S}} > 0$ between any transmit and any receive antenna to any scattering object, that is

$$\|\mathbf{r}_{\mathrm{k}} - \mathbf{r}_m\| \geq d_{\mathrm{S}} \quad \forall k \in \mathcal{T} \cup \mathcal{R},\ \forall m \in \mathcal{S}\,, \tag{34}$$

with a bounded clustering factor, that is, $\gamma < \infty$, and a finite number of scattering objects, that is, $M = |\mathcal{S}| < \infty$. This condition is straight forward to fulfill in any simulation scenario, by introducing an empty region with radius d_{S} around all BS and user antennas in which no scattering object is placed.

While the optimization problem (32) does not assume a specific geometry, we now specialize upper and lower bounds on $|u(\mathbf{r}_{\mathrm{S}})|$ for the case of a circular sector with opening angle θ, as shown in Fig. 8. The user is placed at a distance R from the BS at an angle of $\zeta/2$ from the sector center where we assume $\zeta < \theta$.

The two distances, from the BS to the scattering object and from the scattering object to the user, have to add up to at least R according to the triangle inequality. Therefore, the minimum product of these two distances is obtained, when either of these numbers attains its minimum value d_{S}. As the distances have to add up to R, the other distance is $R - d_{\mathrm{S}}$. This corresponds to the case when the scattering object is located directly at the border of the empty region with radius d_{S}, see positions $\mathbf{r}_{\min}^{(1)}$ and $\mathbf{r}_{\min}^{(2)}$ in Fig. 8. Therefore the solution to the minimization is given by

$$\xi_{\min} = d_{\mathrm{S}}\,(R - d_{\mathrm{S}})\,. \tag{35}$$

Changing (32) to a maximization problem, the product of the distances, from the BS to the scattering object and from the scattering object to the user, is at its maximum, if they both

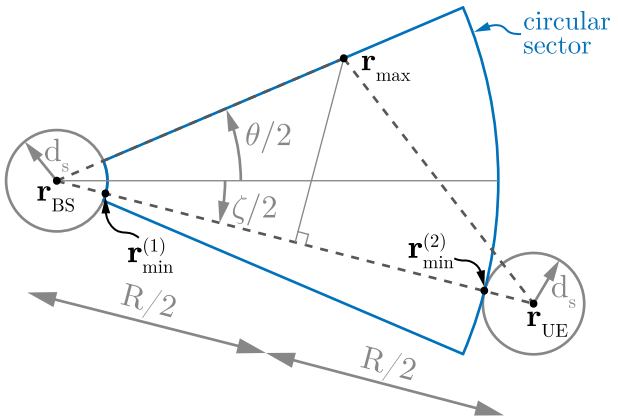

FIGURE 8. Geometry for a circular sector scenario. The scattering object positions $\mathbf{r}^{(1)}_{\min}$ and $\mathbf{r}^{(2)}_{\min}$ lead to a minimum product of distances while a scattering object position $\mathbf{r}_{\max}$ leads to a maximum product of distances.

attain the same maximal value within their possible range. In the case of a circular sector, this corresponds to the case when the scattering object is located at the border of the sector, such that the distances $\|\mathbf{r}_{\mathrm{BS}} - \mathbf{r}_{\mathrm{S}}\|$ and $\|\mathbf{r}_{\mathrm{UE}} - \mathbf{r}_{\mathrm{S}}\|$ are equal and maximal, see position $\mathbf{r}_{\max}$ in Fig. 8. Via elementary geometry, we obtain the solution to the maximization problem as

$$\xi_{\max} = \frac{R^2}{4\cos(\frac{\zeta+\theta}{2})^2}$$
$$\text{for } 0 < \zeta + \theta \leq 2\arccos\left(\frac{R}{2(R-d_{\mathrm{S}})}\right). \tag{36}$$

This leads to the upper and lower bounds on the absolute value of the sum terms:

$$\frac{4\cos(\frac{\theta}{2})^2}{R^2} \leq |u(\mathbf{r}_{\mathrm{S}})| \leq \frac{1}{d_{\mathrm{S}}(R-d_{\mathrm{S}})}. \tag{37}$$

Equation (32) can be solved straight forward for other geometries. We focus on a circular sector geometry in this work.

APPENDIX C
UPPER BOUND ON THE SNR WITH ZF PRECODING

In this section, we provide an upper bound on the SNR (25), obtained by ZF precoding. Due to the similarity invariance of the tr $(\cdot)$ operator, we obtain

$$\mathrm{SNR} = \frac{P_T}{\sigma_w^2}\frac{1}{\mathrm{tr}\left(\left(\mathbf{H}^{\mathrm{H}}\mathbf{H}\right)^{-1}\right)} = \frac{P_T}{\sigma_w^2}\frac{1}{\sum_{k=1}^{U}\frac{1}{\lambda_k}}, \tag{38}$$

where λ_k for $k \in \{1,\ldots,U\}$ denote the eigenvalues of the non-singular matrix $\mathbf{H}^{\mathrm{H}}\mathbf{H}$. Let λ_1 denote the smallest eigenvalue of $\mathbf{H}^{\mathrm{H}}\mathbf{H}$. The channel matrix $\mathbf{H}$ consists of users' channel vectors, that is, $\mathbf{H} = (\mathbf{h}_1,\ldots,\mathbf{h}_U)$. A user's channel vector is given by $\mathbf{h}_k = \sqrt{\eta_k}\tilde{\mathbf{h}}_k$ for $k \in \{1,\ldots,U\}$ where $\eta_k > 0$ denotes the large scale fading coefficient of user k and $\tilde{\mathbf{h}}_k$ describes the small scale fading with $\|\tilde{\mathbf{h}}_k\| = 1\ \forall k$. Through the Min-max Theorem by Courant and Fischer [34] we know

$$\lambda_1 = \min_{\|\mathbf{x}\|=1} \mathbf{x}^{\mathrm{H}}\mathbf{H}^{\mathrm{H}}\mathbf{H}\mathbf{x}. \tag{39}$$

Choosing a vector $\mathbf{v} = \frac{1}{\sqrt{2}}\left(\mathbf{e}_i + e^{i\varphi}\mathbf{e}_j\right)$ where $\mathbf{e}_i$ is a vector with a 1 in the i$^{\text{th}}$ entry and 0s elsewhere, we find an upper bound on the smallest eigenvector as

$$\begin{aligned}\lambda_1 &\leq \min_{\mathbf{v}} \mathbf{v}^{\mathrm{H}}\mathbf{H}^{\mathrm{H}}\mathbf{H}\mathbf{v}\\ &= \min_{i,j,\varphi}\frac{1}{2}\big(\eta_i\tilde{\mathbf{h}}_i^{\mathrm{H}}\tilde{\mathbf{h}}_i + \eta_j\tilde{\mathbf{h}}_j^{\mathrm{H}}\tilde{\mathbf{h}}_j\\ &\quad + \sqrt{\eta_i\eta_j}e^{i\varphi}\tilde{\mathbf{h}}_i^{\mathrm{H}}\tilde{\mathbf{h}}_j + \sqrt{\eta_i\eta_j}e^{-i\varphi}\tilde{\mathbf{h}}_j^{\mathrm{H}}\tilde{\mathbf{h}}_i\big)\\ &= \min_{\substack{i,j\\ i\neq j}}\frac{\eta_i+\eta_j}{2} - \sqrt{\eta_i\eta_j}\left|\tilde{\mathbf{h}}_i^{\mathrm{H}}\tilde{\mathbf{h}}_j\right|,\end{aligned}$$

with $\varphi = \pi - \mathrm{Arg}\left(\tilde{\mathbf{h}}_i^{\mathrm{H}}\tilde{\mathbf{h}}_j\right)$. In the case of equal large scale fading for all users, that is, for $\eta_k = \eta\ \forall k$, we obtain

$$\lambda_1 \leq \eta\left(1 - \max_{\substack{i,j\\ i\neq j}}\left|\tilde{\mathbf{h}}_i^{\mathrm{H}}\tilde{\mathbf{h}}_j\right|\right). \tag{40}$$

Since $\sum_{k=1}^{U}\frac{1}{\lambda_k} > \frac{1}{\lambda_1}$, we obtain an upper bound on the SNR as

$$\mathrm{SNR} \leq \frac{\eta P_T}{\sigma_w^2}\left(1 - \max_{\substack{i,j\\ i\neq j}}\left|\tilde{\mathbf{h}}_i^{\mathrm{H}}\tilde{\mathbf{h}}_j\right|\right). \tag{41}$$

REFERENCES

[1] F. Rusek, D. Persson, B. K. Lau, E. G. Larsson, T. L. Marzetta, O. Edfors, and F. Tufvesson, "Scaling up MIMO: Opportunities and challenges with very large arrays," *IEEE Signal Process. Mag.*, vol. 30, no. 1, pp. 40–60, Jan. 2013.
[2] H. Q. Ngo, E. G. Larsson, and T. L. Marzetta, "Aspects of favorable propagation in massive MIMO," in *Proc. EUSIPCO*, Lisbon, Portugal, Sep. 2014, pp. 76–80.
[3] E. Björnson, E. G. Larsson, and T. L. Marzetta, "Massive MIMO: Ten myths and one critical question," *IEEE Commun. Mag.*, vol. 54, no. 2, pp. 114–123, Feb. 2016.
[4] E. Björnson, J. Hoydis, and L. Sanguinetti, "Massive MIMO networks: Spectral, energy, and hardware efficiency," *Found. Trends Signal Process.*, vol. 11, nos. 3–4, pp. 154–655, 2017.
[5] D.-S. Shiu, G. J. Foschini, M. J. Gans, and J. M. Kahn, "Fading correlation and its effect on the capacity of multielement antenna systems," *IEEE Trans. Commun.*, vol. 48, no. 3, pp. 502–513, Mar. 2000.
[6] C.-M. Chen, V. Volskiy, A. Chiumento, L. Van der Perre, G. A. E. Vandenbosch, and S. Pollin, "Exploration of user separation capabilities by distributed large antenna arrays," in *Proc. IEEE Globecom Workshops*, Washington, DC, USA, Dec. 2016, pp. 1–6.
[7] M. Z. Aslam, Y. Corre, E. Bjoernson, and Y. Lostanlen, "Massive MIMO channel performance analysis considering separation of simultaneous users," in *Proc. ITG WSA*, Bochum, Germany, Mar. 2018, pp. 1–6.
[8] J. Flordelis, F. Rusek, X. Gao, G. Dahman, O. Edfors, and F. Tufvesson, "Spatial separation of closely-located users in measured massive MIMO channels," *IEEE Access*, vol. 6, pp. 40253–40266, 2018.
[9] C. Wang and R. D. Murch, "Adaptive downlink multi-user MIMO wireless systems for correlated channels with imperfect CSI," *IEEE Trans. Wireless Commun.*, vol. 5, no. 9, pp. 2435–2446, Sep. 2006.
[10] T. Van Chien, C. Mollén, and E. Björnson, "Large-scale-fading decoding in cellular massive MIMO systems with spatially correlated channels," 2018, *arXiv:1807.08071*. [Online]. Available: https://arxiv.org/abs/1807.08071

[11] X. Q. Gao, B. Jiang, X. Li, A. B. Gershman, and M. R. McKay, "Statistical eigenmode transmission over jointly correlated MIMO channels," *IEEE Trans. Inf. Theory*, vol. 55, no. 8, pp. 3735–3750, Aug. 2009.

[12] Ö. Özdogan, E. Björnson, and E. G. Larsson, "Uplink spectral efficiency of massive MIMO with spatially correlated Rician fading," in *Proc. SPAWC*, Kalamata, Greece, Jun. 2018, pp. 216–220.

[13] P. Kyösti, J. Meinilä, L. Hentilä, X. Zhao, T. Jämsä, C. Schneider, M. Narandžić, M. Milojević, A. Hong, J. Ylitalo, V.-M. Holappa, M. Alatossava, R. Bultitude, Y. de Jong, and T. Rautiainen, "WINNER II channel models," WINNER, Tech. Rep. IST-4-027756 WINNER II, Deliverable D1.1.2 V1.2, Sep. 2007.

[14] J. Meinilä, P. Kyösti, L. Hentilä, T. Jämsä, E. Suikkanen, E. Kunnari, and M. Narandžić, "WINNER+ final channel models," WINNER, Tech. Rep. CELTIC/CP5-026, Deliverable D5.3, Jun. 2010.

[15] *Technical Specification Group Radio Access Network; Technical Specification Group Radio Access Network: Spatial Channel Model for Multiple Input Multiple Output (MIMO) Simulations*, document TR 25.996, 3GPP, Jun. 2018.

[16] C.-X. Wang, X. Hong, H. Wu, and W. Xu, "Spatial-temporal correlation properties of the 3GPP spatial channel model and the Kronecker MIMO channel model," *EURASIP J. Wireless Commun. Netw.*, vol. 2007, Feb. 2007, Art. no. 039871.

[17] *Study on 3D Channel Model for LTE*, document TR 36.873, 3GPP, May 2018.

[18] F. Ademaj, M. Taranetz, and M. Rupp, "Implementation, validation and application of the 3GPP 3D MIMO channel model in open source simulation tools," in *Proc. Int. Symp. Wireless Commun. Syst. (ISWCS)*, Brussels, Belgium, Aug. 2015, pp. 721–725.

[19] S. Jaeckel, L. Raschkowski, K. Börner, and L. Thiele, "QuaDRiGa: A 3-D multi-cell channel model with time evolution for enabling virtual field trials," *IEEE Trans. Antennas Propag.*, vol. 62, no. 6, pp. 3242–3256, Jun. 2014.

[20] F. Ademaj, M. Müller, S. Schwarz, and M. Rupp, "Modeling of spatially correlated geometry-based stochastic channels," in *Proc. IEEE 86th Veh. Technol. Conf. (VTC-Fall)*, Toronto, ON, Canada, Sep. 2017, pp. 1–6.

[21] F. Ademaj, S. Schwarz, K. Guan, and M. Rupp, "Ray-tracing based validation of spatial consistency for geometry-based stochastic channels," in *Proc. IEEE 88th Veh. Technol. Conf. (VTC-Fall)*, Chicago, IL, USA, Aug. 2018, pp. 1–5.

[22] L. Lium, C. Oestges, J. Poutanen, K. Haneda, P. Vainikainen, F. Quitin, F. Tufvesson, and P. De Doncker , "The COST 2100 MIMO channel model," *IEEE Wireless Commun.*, vol. 19, no. 6, pp. 92–99, Dec. 2012.

[23] X. Gao, F. Tufvesson, and O. Edfors, "Massive MIMO channels—Measurements and models," in *Proc. Asilomar Conf. Signals, Syst. Comput.*, Pacific Grove, CA, USA, Nov. 2013, pp. 280–284.

[24] M. Zhu. *A Public COST 2100 Channel Model MATLAB Source Code*. Accessed: Feb. 5, 2019. [Online]. Available: https://code.google.com/archive/p/cost2100model/downloads

[25] M. Franceschetti, "Stochastic rays pulse propagation," *IEEE Trans. Antennas Propag.*, vol. 52, no. 10, pp. 2742–2752, Oct. 2004.

[26] M. Franceschetti, J. Bruck, and L. J. Schulman, "A random walk model of wave propagation," *IEEE Trans. Antennas Propag.*, vol. 52, no. 5, pp. 1304–1317, May 2004.

[27] J. Salo, H. M. El-Sallabi, and P. Vainikainen, "Statistical analysis of the multiple scattering radio channel," *IEEE Trans. Antennas Propag.*, vol. 54, no. 11, pp. 3114–3124, Nov. 2006.

[28] T. Pedersen and B. H. Fleury, "A realistic radio channel model based in stochastic propagation graphs," in *Proc. MATHMOD*, Vienna, Austria, 2006, pp. 324–331.

[29] T. Pedersen and B. H. Fleury, "Radio channel modelling using stochastic propagation graphs," in *Proc. ICC*, Glasgow, U.K., Jun. 2007, pp. 2733–2738.

[30] T. Pedersen, G. Steinböck, and B. H. Fleury, "Modeling of reverberant radio channels using propagation graphs," *IEEE Trans. Antennas Propag.*, vol. 60, no. 12, pp. 5978–5988, Dec. 2012.

[31] M. Nakagami, "The *m*-distribution—A general formula of intensity distribution of rapid fading," in *Statistical Methods in Radio Wave Propagation*. Amsterdam, The Netherlands: Elsevier, 1960, pp. 3–36.

[32] N. Czink, B. Bandemer, G. Vazquez-Vilar, L. Jalloul, C. Oestges, and A. Paulraj, "Spatial separation of multi-user MIMO channels," in *Proc. PIMRC*, Tokyo, Japan, Sep. 2009, pp. 1059–1063.

[33] M. Skolnik, *Introduction to Radar Systems*, 2nd ed. New York, NY, USA: McGraw-Hill, 1981.

[34] G. H. Golub and C. F. Van Loan, *Matrix Computations*, vol. 3. Baltimore, MD, USA: JHU Press, 2012.

STEFAN PRATSCHNER received the B.Sc. degree in electrical engineering and the M.Sc. degree (Hons.) in telecommunications from TU Wien, Austria, in 2014 and 2016, respectively, where he is currently pursuing the Ph.D. degree with the Institute of Telecommunications and has been a Project Assistant, since 2013. His current research interests include massive MIMO technologies for mobile communications, array processing, and testbed measurements.

THOMAS BLAZEK received the B.Sc. degree in electrical engineering and Dipl.Ing. degree (M.Sc. equivalent) in telecommunications from TU Wien, Vienna, Austria, in 2013 and 2015, respectively, where he is currently pursuing the Ph.D. degree in telecommunications engineering and also a University Assistant with the Institute of Telecommunications. From 2013 to 2014, he was a member of the Mobile Communications Group, TU Wien, where he was involved in system level LTE simulations. His current research interests include modeling and analysis of vehicular channels and measurement testbed design.

ERICH ZÖCHMANN received the B.Sc., Dipl.Ing. (M.Sc.), and Dr.Techn. degrees (Hons.) in electrical engineering from TU Wien, in 2013, 2015, and 2019, respectively. From 2013 to 2015, he was a Project Assistant with the Institute of Telecommunications, where he co-developed the Vienna LTE-A uplink link level simulator and conducted research on physical layer signal processing for 4G mobile communication systems. From 2017 to 2018, he was a Visiting Scholar with The University of Texas at Austin. His current research interests include experimental characterization and modeling of millimeter-wave propagation, physical layer signal processing, array signal processing, compressed sensing, and convex optimization.

FJOLLA ADEMAJ received the M.Sc. degree (Hons.) in telecommunications from the Faculty of Electrical and Computer Engineering, Kosovo, University of Prishtina, in 2014. She is currently pursuing the Ph.D. degree in telecommunications engineering with the Institute of Telecommunications, TU Wien. Her research interests include system level modeling, channel modeling in three dimensions, and evaluation of full-dimension MIMO.

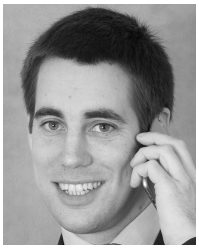

SEBASTIAN CABAN received the master's degree in business administration from the University of Vienna, Vienna, Austria, and the master's and Ph.D. degrees in telecommunications from TU Wien. His current research interest includes measurements in wireless communications.

STEFAN SCHWARZ received the Dipl.-Ing. degree in electrical engineering, the Dr. Techn. degree in telecommunications engineering, and the Habilitation degree in mobile communications from the Vienna University of Technology (TU Wien), in 2009, 2013, and 2019, respectively, where he currently holds a tenure track position at the Institute of Telecommunications and is the Head of the Christian Doppler Laboratory for Dependable Wireless Connectivity for the Society in Motion. His research interests include wireless communications channel modeling, signal processing, and optimization.

MARKUS RUPP received the Dipl.-Ing. degree from the University of Saarbräcken, Germany, in 1988, and the Dr. Ing. degree from the Technische Universität Darmstadt, Germany, in 1993. Until 1995, he held a Postdoctoral position at the University of California at Santa Barbara, Santa Barbara, CA, USA. From 1995 to 2001, he was with the Wireless Technology Research Department, Nokia Bell Labs, Holmdel, NJ, USA. Since 2001, he has been a Full Professor of digital signal processing in mobile communications with TU Wien.